

# Method of Detection Optimization Based on Vector Electric Field Multi-electrode Gradient Information

Jianjun Liu, Chao Wu, Guoyu Cui, Zheng Wang, Yubo Wang, Guofeng Pan, Guohua Liu, Chengbo Hu, Yongling Lu and Xujie He

## 1 Introduction

In the operation of power system, substation operation and maintenance of the substation bear the operation and maintenance management, switching operation and accident handling and other important work, that is to ensure grid security, stability and economic performance of the executor [1]. In the substation operation environment, it is very difficult to calculate the electric field around the space for complicated substation equipment layout. Currently according to the characteristics of the three-dimensional distribution of electric field. In this paper powered equipment is simply treated to calculate the distribution of power-frequency electrical equipment around the distribution with the calculation method of partition segment processing [1]. Because the result accuracy is not high and the method cannot carry on the field strength data real-time computation in the course of moving the job. In this paper, a new detection method combining scene 3D and vector electric field gradient information is proposed, which can realize accurate detection of voltage level, distance and azimuth. This method realizes the accurate detection

---

J. Liu (✉) · C. Wu · G. Cui · Z. Wang · Y. Wang · G. Liu · X. He  
State Grid Key Laboratory of Power Industrial Chip Design and Analysis Technology,  
Beijing Smart-Chip Microelectronics Technology Co., Ltd, C-3, Dongsheng Science  
and Technology Park, No.66, Xixiaokou Rd, Haidian District, Beijing, China  
e-mail: liujianjun@sgitg.sgcc.com.cn

G. Pan  
Microelectronics Technology Institute, Hebei University of Technology,  
No.27 Guangrong Road, Hongqiao District, Tianjin, China  
e-mail: pgf@hebut.edu.cn

C. Hu · Y. Lu  
Jiangsu Electric Power Research Institute, No.1, Pawier Road,  
Jiangning District, Nanjing, Jiangsu, China  
e-mail: 15105182955@163.com

of the voltage level information by acquiring the field strength information of the surrounding live equipment and using the multi-directional electrode gradient detection method to process the collected raw data. At the same time the method of calculating the electric field detection is optimized by using the compression—aware greedy reconstruction algorithm so as to improve the accuracy of the electric field gradient voltage level detection judgment.

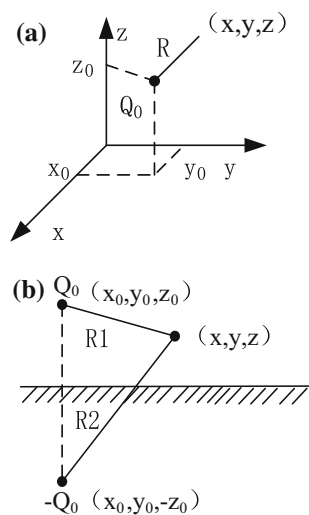
## 2 Principle of Near-Field Detection

The commonly used calculation method of the power frequency electric field intensity of the bus-bar and the surrounding electric equipment is to derive the three-dimensional charge system and the electric field coefficient of the working environment of the surrounding charged body using the simulated charge method [2]. Figure 1 shows the Cartesian coordinate system when calculating the power frequency electric field. Considering the ground effect, the image charge method is used. The asymmetric mirror image method is used without considering the influence of the earth. This paper assumes that the simulated charge coordinate is  $Q_0 (x_0, y_0, z_0)$ .

When the influence of the earth is not considered, this paper takes the coordinate point  $(x, y, z)$ . The point of charge is evaluated from the relation:

$$V = \frac{Q_0}{4\pi\epsilon R} \quad (1)$$

**Fig. 1** Cartesian coordinate system **a** coordinate when mirroring is not considered **b** coordinate when mirroring is considered



The potential coefficient of a single point charge:

$$P = \frac{1}{4\pi\epsilon R} \quad (2)$$

$$R = \sqrt{(x - x_0)^2 + (y - y_0)^2 + (z - z_0)^2}$$

After the simulation of electric charge it can be determined at any point within the region of  $a$  electric field strength:

$$\mathbf{E} = -\nabla V = -\sum_{a=1}^n (\nabla P_{a0}) Q_0 = \sum_{a=1}^n F_{a0} Q_0 \quad (3)$$

$N$  is the number of simulated charges,  $F_{a0}$  is the electric field intensity vector coefficient.

According to the above situation, single point charge electric field strength coefficient is calculated using the following formulas:

$$F_x = -\frac{\partial p}{\partial x} = \frac{1}{4\pi\epsilon} \frac{x - x_0}{R^3} \quad (4)$$

$$F_y = -\frac{\partial p}{\partial y} = \frac{1}{4\pi\epsilon} \frac{y - y_0}{R^3} \quad (5)$$

$$F_z = -\frac{\partial p}{\partial z} = \frac{1}{4\pi\epsilon} \frac{z - z_0}{R^3} \quad (6)$$

When the impact of the earth is taken into account, the spatial region at any point  $(x, y, z)$  potential and strength coefficient:

$$V = \frac{Q_0}{4\pi\epsilon} \left( \frac{1}{R_1} - \frac{1}{R_2} \right) \quad (7)$$

$$P = \frac{1}{4\pi\epsilon} \left( \frac{1}{R_1} - \frac{1}{R_2} \right) \quad (8)$$

Electric field intensity factor:

$$F_x = -\frac{\partial p}{\partial x} = \frac{1}{4\pi\epsilon} \left( \frac{x - x_0}{R_1^3} - \frac{x - x_0}{R_2^3} \right) \quad (9)$$

$$F_y = -\frac{\partial p}{\partial y} = \frac{1}{4\pi\epsilon} \left( \frac{y - y_0}{R_1^3} - \frac{y - y_0}{R_2^3} \right) \quad (10)$$

$$F_z = -\frac{\partial p}{\partial z} = \frac{1}{4\pi\epsilon} \left( \frac{z - z_0}{R_1^3} - \frac{z - z_0}{R_2^3} \right) \quad (11)$$

$$R_1 = \sqrt{(x - x_0)^2 + (y - y_0)^2 + (z - z_0)^2} \quad R_2 = \sqrt{(x - x_0)^2 + (y - y_0)^2 + (z + z_0)^2}$$

CSM could simulate the field strength of the power frequency field generated by the bus, but cannot well simulate field strength of insulator and suspension conductor equipment in substation. Boundary element method (BEM) can solve the problem of bracketing, which can reduce the dimension of the problem and improve the accuracy of the calculation when comparing the field strength of the substation equipment [3, 4].

In this paper, CSM and BEM algorithm are combined to calculate the field strength of the charged carriers in the substation; CSM is used to simulate the field strength generated by the bus. BEM is used to simulate the field strength generated by other equipment in substation.

## 2.1 The Establishment of Simulated Charge Equations

The (electrode)  $n$  analog charge points  $Q_j$  ( $j = 1, 2, \dots, n$ ) is setted outside field;  $N$  potential matching points are selected on the electrode surface of a given potential boundary condition that the potential value  $\varphi_{0j}$  ( $j = 1, 2, \dots, n$ ) on each matching point is known [5]. According to the superposition theorem, the points corresponding to all  $n$  matching points can be calculated from the following formulas [5]:

$$\begin{cases} P_{11}Q_1 + P_{12}Q_2 + \dots + P_{1n}Q_n = \varphi_{01} \\ P_{21}Q_1 + P_{22}Q_2 + \dots + P_{2n}Q_n = \varphi_{02} \\ \dots \\ P_{n1}Q_1 + P_{n2}Q_2 + \dots + P_{nn}Q_n = \varphi_{0n} \end{cases} \quad (12)$$

$P_{ij}$  called potential coefficients is the potential value produced by the  $j$ -th unit charge at the  $i$ -th matching point, which is related to the type and position of the  $j$ -th analog charge and the dielectric constant of the  $i$ -th matching point. but regardless of the charge value of the  $j$ -th analog charge. When the electric field data of the charged object in the substation is calculated, the charge value of the simulated charge can be calculated by Gaussian column principal component elimination method  $Q_j$  ( $j = 1, 2, \dots, n$ ) [6].

## 2.2 The Verification and Determination of Analog Charge Value

The simulated charge data can not directly calculate the potential or electric field strength at any point in the field. It is necessary to check whether the potential generated by these analog charges satisfies the boundary conditions of the non-matching points on the electrode surface [7]. In this paper,  $m$  potential calibration points are selected in the middle of two adjacent points matching points, and the potential of each potential calibration point is calculated with the simulation charge.

$$\varphi_k = P_{k1}Q_1 + P_{k2}Q_2 + \cdots + P_{kn}Q_n \quad (k = 1, 2, \dots, m) \quad (13)$$

$\varphi_k$  ( $k = 1, 2, \dots, m$ ) of each potential checkpoint is compared with a given known potential value  $\varphi_{0k}$  ( $k = 1, 2, \dots, m$ ) to determine whether or not the meeting following condition.

$$|\varphi_k - \varphi_{0k}| \leq \Delta \quad (k = 1, 2, \dots, m) \quad (14)$$

$\Delta$  is the calculation error determined by the operator, the charge value of the simulation charge can be solved by formula (12), and the electric potential or electric field strength can be calculated at any point in the field by applying these analog charges [5]. If formula (14) is not satisfied, the type, position, and number of analog charges for the first hypothesis should be adjusted appropriately and recalculate formulas (12) and (13) until meet formula (14) [7].

## 3 Calculation Method of Electric Field Gradient Based on Algorithm Optimization

In this paper, in order to increase the accuracy of the multi-electrode electric field gradient detection calculation, the pre-processing of the original data of the electric field is increased, and the calculation method of the electric field gradient detection is optimized by using the compression-aware greedy reconstruction algorithm to calculate the voltage level, Distance information [8].

The overall input of the algorithm is the original data collected by the electric field detection collector, which is the electric field raw data collected by 8 multi-electrode multi-position electrode detecting devices.

The overall output of the algorithm is the electric field detection result, including: distance, azimuth, voltage grade information.

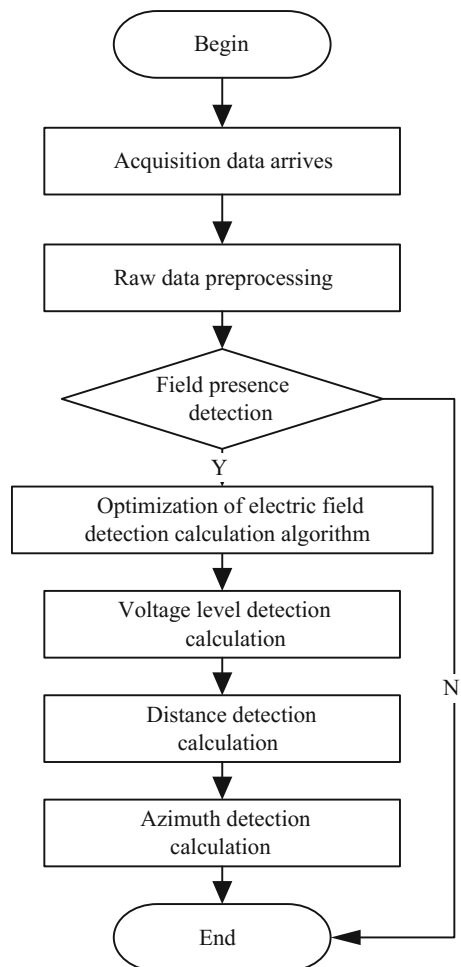
Algorithm design principles: making full use of the advantages and characteristics of multi-electrode detection to detection of electric field strength. In the voltage level detection, according to electric field gradient information generated by

multi-electrode detection equipment, so as to analyze voltage level. The algorithm flow chart shown as Fig. 2:

In Fig. 2 when the field strength detection data frame arrives, data preprocessing is performed first, and then the field strength detection is performed. If the field strength data is null, the algorithm is exited directly, then the next frame data is ready to be processed. If the field strength is found in turn to determine the voltage level, distance calculation, azimuth decision. In the preprocessing section of the field data, individual electrode measurements may be abnormal due to hand touch or other conductors, contact of the charged body, and complex environment. So the singular value detection is used to exclude data abnormal results [9].

In this paper, the spatiotemporal distribution test is used to identify the normal, mutation, trend and abnormal conditions, which can identify the mutation value,

**Fig. 2** Electric field intensity data processing flow



trend value and abnormal value [6]. The main basis for the inspection is based on the comparison of the previous field measurements with the previous measured value, the characteristic value (maximum value, minimum value). So needing to count this  $Y_i$ , the previous measurement  $Y_{i-1}$ ,  $Y_{\max}$  occurred in the maximum and minimum  $Y_{\min}$  [6].

- (1) When the difference between the measured value  $Y_i$  and the previous measured value  $Y_{i-1}$  is greater than 3 times the observed error  $v$ , then the value is the mutation value:

$$|Y_i - Y_{i-1}| \geq 3\sigma \quad (15)$$

- (2) Trend identification: When the measured value and the basic environment of the same amount of the difference between the previous measurement is greater than 3 times the error in observation, the measured trend of change:

$$|Y_i - Y_{i-1}| \geq 3\sigma \quad (16)$$

At this time there is a tendency to change the measured value, the rate of change can be calculated.

- (3) Abnormal value recognition: If  $Y_{\min} \leq Y_i \leq Y_{\max}$ , then the measured value is normal, otherwise abnormal.

In this paper, the compression perception theory is applied to the electric field gradient detection algorithm, which is used to calculate the inverse problem of power frequency electric field. The method requires only a small number of electric field strength monitoring points to be randomly deployed in the monitoring area. The field-source parameters and the field-intensity distribution cloud map are obtained by the compression-aware greedy reconstruction algorithm by the electric field monitoring points randomly arranged in the monitoring area [5]. Simulation results show that the compression-aware greedy reconstruction algorithm can reconstruct the distribution of the intensity distribution. Specific steps are as follows:

- (1) compression sampling process:

Assuming that the sensor node coordinates in the  $m$ -th grid are  $(x_m, y_m)$ . The element  $\Phi \in \mathbf{R}^{M \times N}$  ( $M \ll N$ ) in the measurement matrix  $\varphi_{m,n}$  is:

$$\varphi_{m,n} = \mathbf{E}_{m,n}, \quad 1 \leq m \leq M, \quad 1 \leq n \leq N \quad (17)$$

In the above formula,  $\mathbf{E}_{m,n}$  is the field strength of the simulated charge located in the  $n$ th grid measured by the sensor node in the  $m$ -th grid, and can be obtained by the formula (13).

In this paper, the system's compression sampling process can be described by the following formula:

$$\begin{bmatrix} y_1 \\ y_2 \\ \mathbf{M} \\ y_M \end{bmatrix} = \begin{bmatrix} \mathbf{E}_{1,1} & \mathbf{E}_{1,2} & \mathbf{L} & \mathbf{E}_{1,N} \\ \mathbf{E}_{2,1} & \mathbf{E}_{2,2} & \mathbf{L} & \mathbf{E}_{2,N} \\ \mathbf{M} & \mathbf{M} & & \mathbf{M} \\ \mathbf{E}_{M,1} & \mathbf{E}_{M,2} & \mathbf{L} & \mathbf{E}_{M,N} \end{bmatrix} \begin{bmatrix} x_1 \\ x_2 \\ \mathbf{M} \\ x_N \end{bmatrix} \quad (18)$$

In the above equation,  $x_n = q$  ( $1 \leq n \leq N$ ) when there is an equivalent positive charge  $+q$  in the  $n$ th grid;  $x_n = -q$  ( $1 \leq n \leq N$ ) when there is an equivalent negative charge  $-q$ ; No equivalent charge when  $x_n = 0$ ; Assuming that the equivalent number of simulated charges is  $K$ , the sparse degree of  $N$ -dimensional vector  $\mathbf{X}$  is  $K$ . The measurement result of the sensor  $\mathbf{Y}$  is the product of the measurement matrix and the sparse vector  $\mathbf{X}$ , and the physical meaning of the element  $y_m$  ( $1 \leq m \leq M$ ) of  $\mathbf{Y}$  is the sum of the field strengths of all equivalent analog charges at that point [8].

$$\mathbf{Y}_{M \times 1} = \mathbf{E}_{M \times N} \mathbf{X}_{N \times 1} \quad (19)$$

In the above equation,  $\mathbf{Y}$  represents the compression sampling process, that is,  $\mathbf{Y}$  measurement result process. Compression-aware reconstruction is the process of reconstructing the sparse vector  $\mathbf{E}$  according to  $\mathbf{Y}$  and  $\mathbf{E}$ .

(2) The algorithm of electric field cloud diagram greedy reconstruction

In this paper, the main idea of the design of greedy algorithm is used for the characteristics of the inverse problem of power frequency electric field. The greedy reconstruction algorithm of electric field cloud image is designed by using the analogue charge equivalent model. If the substation equipment parameters and spatial distribution of a priori data, the equivalent charge in the grid position should be further defined to improve algorithm performance and operation speed. Greedy reconstruction algorithm design is shown as below [6]:

Input: Measuring matrix  $\mathbf{E}_{M \times N}$ , measurement result  $\mathbf{Y}_{M \times 1}$ , output: reconstructed signal  $\hat{\mathbf{X}}$ .

- (1) Initializing the matching margin  $\mathbf{y}' = \mathbf{y}$ , reconstructing the results  $\hat{\mathbf{X}} = \mathbf{0}$ , all the grid  $N$  is the number of the support collection;
- (2) The following optimization problem is solved: where  $\mathbf{z}$  is a column vector with sparse degree of 1 (only the  $i$ -th element has the value  $z_i$  and the remaining elements are 0). In this paper, the equivalent electric charge is discretized. The physical meaning is that there are  $z_i$  equivalent unit simulation charges at the  $i$ -th grid, if  $z_i$  is positive,  $z_i$  is positive charge; if  $z_i$  is negative,  $z_i$  is negative charge. If there is a priori knowledge of the equivalent charge distribution, then  $i$  and  $z_i$  need to satisfy the following a priori constraints [10].

$$\mathbf{z} = \arg \max \frac{\langle \mathbf{y}', \mathbf{Ez} \rangle}{\|\mathbf{Ez}\|_2} \quad (20)$$

$$1 \leq i \leq N, \quad -M \leq z_i \leq M$$



- (3) If  $z \neq 0$ , then  $y' = y' - Ez$ ,  $\hat{X} = \hat{X} + z$ , so the support set minus the current grid and jumping to step 2;
- (4) Signal reconstruction ends. The result is  $\hat{X}$ .

In the above algorithm, the approximation and margin updating are carried out by finding the correlation between the residual  $y'$  and each atom in the measurement matrix, to ensure that each iteration is optimal, and the maximum number of iterations is  $N$ .

## 4 Experiment and Analysis of Electric Field Gradient Data Detection

In this paper, 110 kV transformer substation equipment for experiments is selected. The optimized data is processed by the optimized multi-pole electric field gradient detection algorithm. The electric field tester and the Matlab tool are used to compare and analyze the processed data, the results are as follows:

A live carrier of 110 kV substation is selected and Charged field electric field gradient data are processed by the above-mentioned optimization algorithm. The cross-section is obtained. The field distribution of X-axis and Y-axis are shown as Figs. 3, 4 and 5. The carrier equipment is 1.5 m above the ground. The X-axis ranges from  $-3.3$  to  $3.3$  m and the Y-axis ranges from  $-7.5$  to  $7.5$  m. The origin is at the center of the interval, and the Z-axis represents the magnitude of the field strength in units of V/m.

**Fig. 3** Field strength distribution of 110 kV substation

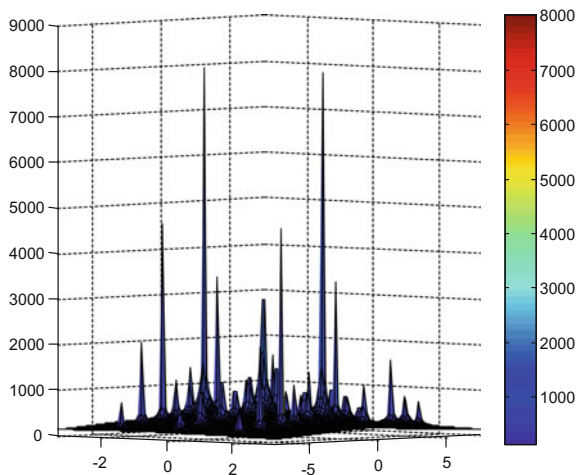


**Fig. 4** Field strength distribution of 110 kV substation with X-axis angle

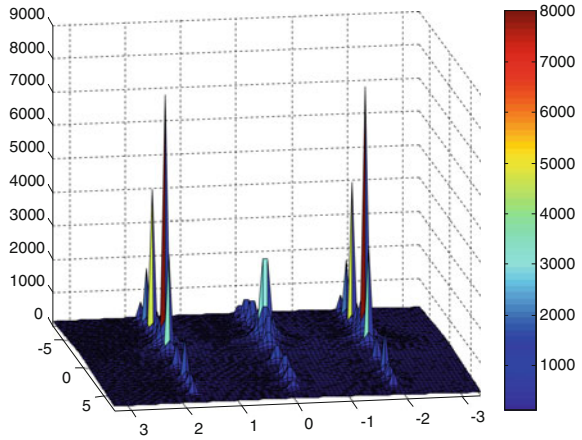
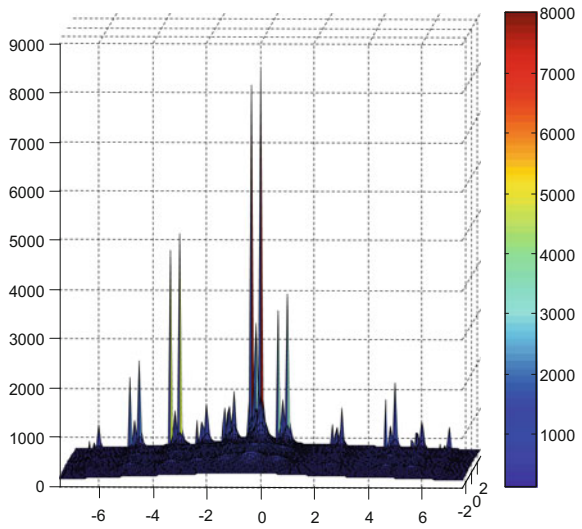


**Fig. 5** Field distribution of 110 kV substation in Y-axis direction



In Figs. 3, 4 and 5, the result of three—dimensional field strength simulation shows that due to the mutual offset effect of the superposition field strength, the maximum field strength appears near the middle position.

Through detecting the field intensity distribution from the same direction in different directions, the result shows that the gradients can only be identified by the multi-layer electrode stacking, and the gradient recognition can be realized only for single-level sensors. The biggest advantage is the ability to determine the voltage level.

In this paper, the greedy matching algorithm (GMP) is simulated in Matlab according to the data parameters shown in Table 1. The results of the different reconstruction algorithms shown in Fig. 6 are obtained, by comparing the

**Table 1** Main simulation data parameters

Simulation parameters	Parameter variable	Parameter value
The divided number of meshes	N	196
Number of sensors	M	49
The number of simulated charges	K	1-20

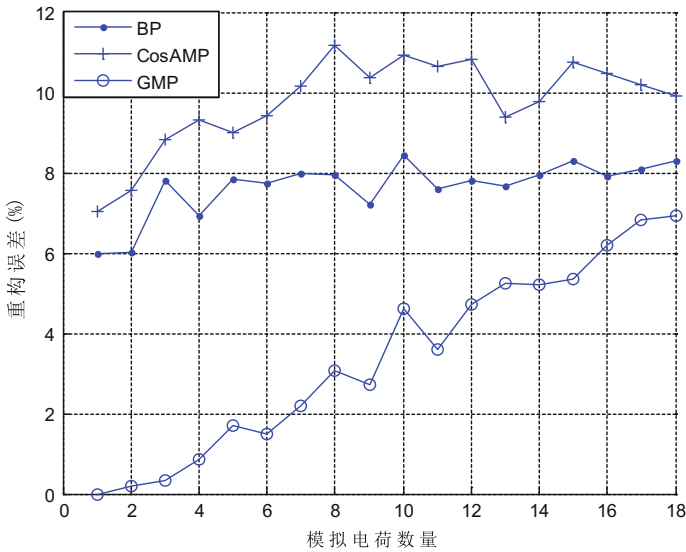


**Fig. 6** Reconstruction error comparison of different reconstruction algorithms

simulation results with the BP (L1-Magic) algorithm [11] and the CosAMP algorithm. In the simulation process, the selected monitoring area is  $50\text{ m} \times 50\text{ m}$  rectangular area, the simulation parameters are selected as shown in Table 1. General requirement is  $M > 2K$ , the best is  $4K \sim 6K$ , the original signal can be a better reconstruction [11].

The results show that compared with the reconstruction error term of BP (L1-Magic) algorithm [11], CosAMP algorithm and the greedy matching algorithm (GMP) proposed in this paper, under the condition of  $M = 49$ ,  $K = 1-18$ ,  $\text{SNR} = 20\text{ dB}$ , the improved compression perception greedy reconstruction algorithm (GMP) can improve the accuracy of reconstruction error. For the 196 grid, the compression-aware greedy reconstruction algorithm can reconstruct the distribution of the source parameters and the distribution of the field strength with only 49 measurements.

## 5 Conclusion

In this paper, the method of calculating the gradient information of multi-electrode electric field is optimized by combining the idea of compression-conscious reconstruction, the original data is preprocessed at the initial stage of the electric field information collection of the charged carrier in the substation. The results are verified by using the electric field strength detection tool and Matlab simulation shows that the optimization algorithm of multi-electrode electric field gradient information detection and analysis, which incorporates the idea of compression perception and reconstruction, can effectively improve the detection ability of the charged conductor voltage level and the response speed and accuracy of the electric field around the charged body, and improve the safety of the staff working in the environment of complex electric field environment.

**Acknowledgements** State Grid Corporation of Science and Technology Project (526816160024).

## References

1. Lee BY, Park JK, Myung SH, Min SW, Kim ES (1997) An effective modelling method to analyze the electric field around transmission lines and substations using a generalized finite line charge. *IEEE Trans Power Delivery* 12(3):1143–1150
2. Takuma T, Ikeda T, Kawamoto T (1981) Calculation of ion flow fields of hvdc transmission lines by the finite element method. *IEEE Power Eng Rev PAS-100(12)*:4802–4810
3. Takuma T, Kawamoto T (1987) A very stable calculation method for ion flow field of hvdc transmission lines. *IEEE Trans Power Delivery* 2(1):189–198
4. Krajewski W (2004) Numerical modelling of the electric field in HV substations. *IEE Proceedings-Science, Meas Technol* 151(4):267–272
5. Du Z, Ruan J, Gan Z, Ruan X, Rong R, Nie L et al (2012) Three-dimensional numerical simulation of power frequency electromagnetic field inside and outside substation. *Power Syst Technol* 36(4):229–235 (in Chinese)
6. Ye Q, Wen Y, Mo R, Huang T, Zhang G, Liu X et al (2012) Calculation of power frequency electromagnetic field within substation by moment method and actual measured results. *Power Syst Technol* 36(2):189–194 (in Chinese)
7. Li N, Peng Z, Du J, Fan C (2012) Simulate calculation and distribution of power frequency electric filed in uhv substations. *High Voltage Eng* 38(9):2178–2188 (in Chinese)
8. Fisch D, Gruber T, Sick B (2011) Swiftrule: mining comprehensive classification rules for time series analysis. *IEEE Trans Knowl Data Eng* 23(5):774–787
9. Candes EJ, Romberg J, Tao T (2004) Robust uncertainty principles: exact signal reconstruction from highly incomplete frequency information. *IEEE Trans Inf Theory* 52(2):489–509
10. Tropp JA, Wright SJ (2009) Computational methods for sparse solution of linear inverse problems. *Proc IEEE* 98(6):948–958
11. Zhu Y, Yin J (2013) Study on application of multi-kernel learning relevance vector machines in fault diagnosis of power transformers. *Proc Csee* 33(22):68–74 (in Chinese)